



HAL
open science

A very high-order finite volume method for the one dimensional convection diffusion problem

Stéphane Clain, Gaspar Machado, Rui M. S. Pereira

► **To cite this version:**

Stéphane Clain, Gaspar Machado, Rui M. S. Pereira. A very high-order finite volume method for the one dimensional convection diffusion problem. 2011. hal-00653968

HAL Id: hal-00653968

<https://hal.science/hal-00653968>

Preprint submitted on 20 Dec 2011

HAL is a multi-disciplinary open access archive for the deposit and dissemination of scientific research documents, whether they are published or not. The documents may come from teaching and research institutions in France or abroad, or from public or private research centers.

L'archive ouverte pluridisciplinaire **HAL**, est destinée au dépôt et à la diffusion de documents scientifiques de niveau recherche, publiés ou non, émanant des établissements d'enseignement et de recherche français ou étrangers, des laboratoires publics ou privés.

A very high-order finite volume method for the one dimensional convection diffusion problem

S. Clain^{a,b}, G. Machado^a, R. M. S. Pereira^a

^a *Departamento de Matemática e Aplicações and Centro de Matemática, Campus de Azurém - 4800-058 Guimarães, Portugal*

^b *Institut de Mathématiques de Toulouse, Université de Toulouse, France*

Abstract

A new finite volume method for one dimensional convection diffusion problems is designed. The scheme is based on the Polynomial Reconstruction Operator (PRO-scheme) where a 5-degree polynomial representation is provided for each cell using the mean-values of the neighboring cells. Convective and diffusive numerical fluxes derive from the polynomial reconstruction and lead to a finite volume scheme of sixth-order of accuracy. Numerical examples are proposed to show the effectiveness of the method and the ability to manage the convection and the diffusion independently, *i.e.* the scheme is still functional even with vanishing viscosity.

Keywords: Finite Volume, very high-order, convection-diffusion, Polynomial Reconstruction Operator (PRO).

1. Introduction

Efficient numerical schemes to solve convection diffusion equations is a constant challenge due to the wide range of problems which concern the coupling of the two major physical phenomena. Finite difference and finite element methods are very popular to produce numerical approximations ([5, 16, 22]) and a lot of academic or commercial codes are based on such techniques. The finite volume method for convection diffusion equations has been introduced in the sixties [20, 21] but do not received attention during three decades whereas the finite element method has known a wide

Email addresses: `clain@math.uminho.pt` (S. Clain), `gjm@math.uminho.pt` (G. Machado), `rmp@math.uminho.pt` (R. M. S. Pereira)

Preprint submitted to Elsevier

December 20, 2011

expansion. In the early eighties, the FV method was brought to the fore with the original book of Patankar [19] for structured meshes and widely employed by engineers or physicists. Indeed, the method appears to be an interesting alternative due to its simplicity (one information per cell), the built-in conservative property, and the capacity to handle unstructured and non-conformal meshes. Important developments have been realised in this way and several classes of methods have been proposed. First, the original Patankar scheme for structured meshes has been extended to the non-structured case where an orthogonality condition is required to allow admissible diffusion flux (FV4 scheme [2, 3, 14, 13]). The diamond scheme based on a local reconstruction of the gradient on each edge has been introduced by [8, 9, 18] while a finite volume scheme based on primal and dual meshes (DDFV scheme) has been proposed and developed by [17, 12, 10]. In the last six years, new techniques to design efficient finite volume schemes has been realised and a large proposal of numerical algorithms is now available such as the mixed-hybrid schemes [11, 15] or mimetic schemes [1, 4].

Despite a constant effort to improve the schemes, a serious drawback of the finite volume method is the large amount of numerical viscosity and the weak convergence rate (at most second-order convergence). In the finite volume context, mean values are the fundamental data and the traditional (and implicit) identification "mean values = point-wise value at centroid" used by most of the authors is responsible of the discrepancy leading to, at most, a second-order scheme. The fact to reject such an identification is the crucial aspect of the method to provide sixth-order accuracy schemes. The main tool of the method is a local polynomial reconstruction in which the coefficients are determined from the mean values of the neighboring cells [6, 7]. Another important point is the choice of the reconstruction in function of the operator. For the convective part, we only employ internal values, *i.e.* mean-values on the cells, to determine the reconstructed polynomial function whereas we introduce the Dirichlet conditions in the polynomial reconstruction employed in the diffusive contribution to enforce the boundary conditions.

This paper is devoted to a new class of finite volume schemes for steady-state convection-diffusion problem able to reach the sixth-order accuracy in space. We present the method for the one-dimensional case to detail the scheme with simple examples considering the convection-diffusion equation

in the domain $\Omega :=]0, 1[$ with Dirichlet boundary conditions

$$\begin{aligned} - (au')' + (vu)' &= f \quad \text{on } \Omega \\ u(0) &= u_{\text{lf}}, \quad u(1) = u_{\text{rg}}, \end{aligned}$$

where we assume that a and v are regular functions on $\bar{\Omega}$ with $a(x) \geq \alpha > 0$ for all $x \in \Omega$ while f represents a regular source term. Extension for two- and three-dimensional geometries is under study.

The rest of the paper is as follows. The second section recalls the classical finite volume scheme for convection-diffusion problem (namely the Patankar method). Then, we introduce several polynomial reconstructions in section three, while the fourth section is devoted to the high-order finite volume schemes. The last section concerns the numerical tests to show the scheme capacity to provide sixth-order accuracy both for the convective and the diffusive part of the operator.

2. Patankar finite volume schemes

To design the numerical schemes, we denote by \mathcal{T}_h a mesh of Ω constituted of cells $K_i := [x_{i-1/2}, x_{i+1/2}]$, $i = 1, \dots, I$, of centroid c_i , where $x_{1/2} := 0$ and $x_{i+1/2} := x_{i-1/2} + h_i$, and set h_r as the ratio between the length of two consecutive cells, that is $h_r := \frac{h_i}{h_{i+1}}$, $i = 1, 3, \dots, I - 1$ (*cf.* Fig. 1).

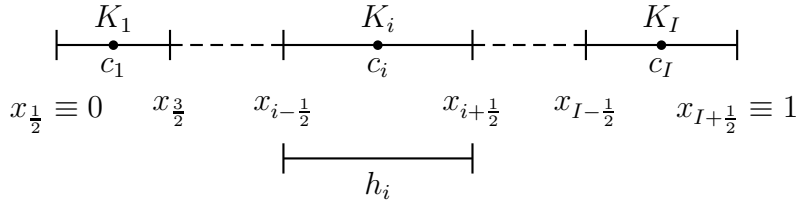


Figure 1: Mesh, cells and interface notations

In the finite volume context, u_i denotes an approximation of the mean value over cell K_i , that is $u_i \approx \frac{1}{h_i} \int_{K_i} u(x) dx$. For the sake of consistency, we recall that the Patankar scheme for each cell K_i , $i = 1, \dots, I$, is given

by

$$\begin{aligned}
& - \left[\mathcal{F}_{d,i+\frac{1}{2}}^{\mathcal{P}}(u_i, u_{i+1}) - \mathcal{F}_{d,i-\frac{1}{2}}^{\mathcal{P}}(u_{i-1}, u_i) \right] \\
& + \left[\mathcal{F}_{c,i+\frac{1}{2}}^{\mathcal{P}}(u_i, u_{i+1}) - \mathcal{F}_{c,i-\frac{1}{2}}^{\mathcal{P}}(u_{i-1}, u_i) \right] = h_i f_i,
\end{aligned} \tag{1}$$

where the diffusive and the convective fluxes write

$$\mathcal{F}_{d,i+\frac{1}{2}}^{\mathcal{P}}(u_i, u_{i+1}) := a(x_{i+\frac{1}{2}}) \frac{2(u_{i+1} - u_i)}{(h_i + h_{i+1})}, \tag{2}$$

$$\mathcal{F}_{c,i+\frac{1}{2}}^{\mathcal{P}}(u_i, u_{i+1}) := [v(x_{i+\frac{1}{2}})]^+ u_i + [v(x_{i+\frac{1}{2}})]^- u_{i+1}, \tag{3}$$

respectively. We have set $h_0 := 0$, $h_{I+1} := 0$, $u_0 := u_{\text{lf}}$, $u_{I+1} := u_{\text{rg}}$, and used the notation $[\alpha]^+ := \frac{\alpha+|\alpha|}{2}$, and $[\alpha]^- := \frac{\alpha-|\alpha|}{2}$. Finally, f_i denotes an approximation of the mean value of f over cell K_i , that is $f_i \approx \frac{1}{h_i} \int_{K_i} f \, dx$.

Equations (1), (2), (3) lead to the linear system

$$A^{\mathcal{P}} U = F + F_{\mathcal{D}},$$

with $U := (u_1, \dots, u_I)^t \in \mathbb{R}^I$ the unknown values, $A^{\mathcal{P}}$ an M-matrix, $F := (h_1 f_1, \dots, h_I f_I)^t \in \mathbb{R}^I$ the source term, and

$$F_{\mathcal{D}} := \left(\left\{ \frac{2a(0)}{h_1} + [v(0)]^+ \right\} u_{\text{lf}}, 0, \dots, 0, \left\{ \frac{2a(1)}{h_I} + [v(1)]^- \right\} u_{\text{rg}} \right)^t \in \mathbb{R}^I$$

the vector collecting the contributions deriving from the Dirichlet boundary conditions. Remark that the finite volume scheme is not equivalent to the finite element scheme or finite difference one for non-uniform meshes.

3. Polynomial reconstruction operators (PRO)

The main tool to provide very high-order approximations is a cute polynomial approximation. In the sequel, we shall consider three kinds of reconstructions. For each cell K_i , $i = 1, \dots, I$, we denote by $\nu(i)$ the stencil associated to cell K_i such that $i \notin \nu(i)$, *i.e.* a set of neighboring cells, and by $u_i(x; \nu(i), \mathbf{d}) \in \mathbb{P}_{\mathbf{d}}$ the polynomial reconstruction on cell K_i of degree \mathbf{d} based on the stencil $\nu(i)$.

In practice, we build the stencil $\nu(i)$ in function of the polynomial degree \mathbf{d} we shall reconstruct picking up the nearest $\mathbf{d} + 1$ cells to K_i . A difficulty arises when dealing with cells which share a point with the boundary. The three proposed reconstructions vary in the manner that the boundary conditions are considered.

3.1. *Design of polynomial $\hat{u}_i(x; \nu(i), \mathbf{d})$*

For each cell K_i , $i = 1, \dots, I$, we consider the polynomial expression (we skip the $\nu(i)$ reference for the sake of simplicity)

$$\hat{u}_i(x; \mathbf{d}) := u_i + \sum_{\alpha=1}^{\mathbf{d}} \hat{\mathcal{R}}_{\alpha}^i \left[(x - c_i)^{\alpha} - \frac{1}{h_i} \int_{K_i} (x - c_i)^{\alpha} dx \right],$$

where the coefficients $\hat{\mathcal{R}}_{\alpha}^i$, $\alpha = 1, \dots, \mathbf{d}$, are the minimizers of the functional

$$\hat{E} \left(\hat{\mathcal{R}}_{\alpha}^i \right) := \sum_{j \in \nu(i)} \left[\frac{1}{h_j} \int_{K_j} \hat{u}_i(x; \mathbf{d}) dx - u_j \right]^2, \quad i = 1, \dots, I.$$

As we shall see, such a reconstruction is well-adapted for the hyperbolic part of the convection diffusion operator.

3.2. *Design of polynomial $\tilde{u}_i(x; \nu(i), \mathbf{d})$*

For each cell K_i , $i = 2, \dots, I - 1$, we use the same polynomial function than above setting $\tilde{\mathcal{R}}_{\alpha}^i := \hat{\mathcal{R}}_{\alpha}^i$ with

$$\tilde{u}_i(x; \mathbf{d}) := u_i + \sum_{\alpha=1}^{\mathbf{d}} \tilde{\mathcal{R}}_{\alpha}^i \left[(x - c_i)^{\alpha} - \frac{1}{h_i} \int_{K_i} (x - c_i)^{\alpha} dx \right].$$

To provide the reconstructed polynomial function for $i = 1$, we slightly modify the functional introducing the boundary condition

$$\tilde{E} \left(\tilde{\mathcal{R}}_{\alpha}^1 \right) := (\tilde{u}_1(0) - u_{\text{lf}})^2 + \sum_{j \in \nu(0)} \left[\frac{1}{h_j} \int_{K_j} \tilde{u}_1(x; \mathbf{d}) dx - u_j \right]^2,$$

where we set $\nu(0) := \nu(1) - \{\text{last cell of } \nu(1)\}$. In the same way, we compute the last polynomial by minimizing functional

$$\tilde{E} \left(\tilde{\mathcal{R}}_{\alpha}^I \right) := \sum_{j \in \nu(I+1)} \left[\frac{1}{h_j} \int_{K_j} \tilde{u}_I(x; \mathbf{d}) dx - u_j \right]^2 + (\tilde{u}_I(1) - u_{\text{rg}})^2,$$

where now we set $\nu(I+1) := \nu(I) - \{\text{first cell of } \nu(I)\}$. We shall see in the sequel that the reconstruction is well-adapted for the elliptic part of the convection diffusion operator.

3.3. Design of polynomial $\check{u}_i(x; \nu(i), \mathbf{d})$

We first define reconstruction $\check{u}_i(x; \mathbf{d}) := \hat{u}_i(x; \mathbf{d})$ for $i = 1, \dots, I$ and add two new polynomial functions for $i = 0$ and $i = I + 1$. For $i = 0$, we set

$$\check{u}_0(x; \mathbf{d}) := u_{\text{lf}} + \sum_{\alpha=1}^{\mathbf{d}} \check{\mathcal{R}}_{\alpha}^0(x-0)^{\alpha},$$

where we determine the coefficients minimizing the functional

$$\check{E}(\check{\mathcal{R}}_{\alpha}^i) := \sum_{j \in \nu(0)} \left[\frac{1}{h_j} \int_{K_j} \check{u}_0(x; \mathbf{d}) dx - u_j \right]^2.$$

In the same way, we set

$$\check{u}_{I+1}(x; \mathbf{d}) := u_{\text{rg}} + \sum_{\alpha=1}^{\mathbf{d}} \check{\mathcal{R}}_{\alpha}^{I+1}(x-1)^{\alpha},$$

where now the coefficients minimize the functional

$$\check{E}(\check{\mathcal{R}}_{\alpha}^{I+1}) := \sum_{j \in \nu(I+1)} \left[\frac{1}{h_j} \int_{K_j} \check{u}_{I+1}(x; \mathbf{d}) dx - u_j \right]^2$$

($\nu(0)$ and $\nu(I+1)$ are the same sets of the previous subsection).

4. Finite volume schemes

The design of the finite volume schemes is based on the Polynomial Reconstruction Operator (PRO-FV-scheme). The diffusive and the convective fluxes for the interior points write

$$\begin{aligned} \mathcal{F}_{\text{d}, i+\frac{1}{2}}(\mathbf{u}_i, \mathbf{u}_{i+1}) &:= a(x_{i+\frac{1}{2}}) \frac{\mathbf{u}'_i(x_{i+\frac{1}{2}}; \mathbf{d}) + \mathbf{u}'_{i+1}(x_{i+\frac{1}{2}}; \mathbf{d})}{2} \quad \text{and} \\ \mathcal{F}_{\text{c}, i+\frac{1}{2}}(\mathbf{u}_i, \mathbf{u}_{i+1}) &:= [v(x_{i+\frac{1}{2}})]^+ \mathbf{u}_i(x_{i+\frac{1}{2}}; \mathbf{d}) + [v(x_{i+\frac{1}{2}})]^- \mathbf{u}_{i+1}(x_{i+\frac{1}{2}}; \mathbf{d}), \end{aligned}$$

$i = 1, \dots, I-1$, respectively, where \mathbf{u} means \check{u} or \tilde{u} or \hat{u} .

Numerical flux at the boundary has to be evaluated as a function of the polynomial reconstruction for $i = 0$ and $i = I+1$ when necessary. For the convective flux, we use the extension $\hat{u}_0 \equiv \tilde{u}_0 := u_{\text{lf}}$ and $\hat{u}_{I+1} \equiv \tilde{u}_{I+1} := u_{\text{rg}}$ when employing reconstructions \hat{u} or \tilde{u} respectively. For the diffusive flux

we set $\tilde{u}_0 := \tilde{u}_1$ and $\tilde{u}_I := \tilde{u}_{I+1}$. It is important to remark that notations \tilde{u}_0 and \tilde{u}_{I+1} have different meanings with respect to the convective flux or the diffusive flux.

Based on the polynomial reconstruction and the definition of the fluxes, we now introduce three affine operators $U \rightarrow G^\alpha(U; u_{\text{lf}}, u_{\text{rg}}, f, \mathbf{d})$, $\alpha = 1, 2, 3$, from \mathbb{R}^I into \mathbb{R}^I given component by component by:

$$G_i^1(U; u_{\text{lf}}, u_{\text{rg}}, f, \mathbf{d}) := - \left[\mathcal{F}_{\text{d}, i+\frac{1}{2}}(\check{u}_i, \check{u}_{i+1}) - \mathcal{F}_{\text{d}, i-\frac{1}{2}}(\check{u}_i, \check{u}_{i+1}) \right] + \left[\mathcal{F}_{\text{c}, i+\frac{1}{2}}(\check{u}_i, \check{u}_{i+1}) - \mathcal{F}_{\text{c}, i-\frac{1}{2}}(\check{u}_i, \check{u}_{i+1}) \right] - h_i f_i, \quad (4)$$

$$G_i^2(U; u_{\text{lf}}, u_{\text{rg}}, f, \mathbf{d}) := - \left[\mathcal{F}_{\text{d}, i+\frac{1}{2}}(\tilde{u}_i, \tilde{u}_{i+1}) - \mathcal{F}_{\text{d}, i-\frac{1}{2}}(\tilde{u}_i, \tilde{u}_{i+1}) \right] + \left[\mathcal{F}_{\text{c}, i+\frac{1}{2}}(\tilde{u}_i, \tilde{u}_{i+1}) - \mathcal{F}_{\text{c}, i-\frac{1}{2}}(\tilde{u}_i, \tilde{u}_{i+1}) \right] - h_i f_i, \quad (5)$$

$$G_i^3(U; u_{\text{lf}}, u_{\text{rg}}, f, \mathbf{d}) := - \left[\mathcal{F}_{\text{d}, i+\frac{1}{2}}(\hat{u}_i, \hat{u}_{i+1}) - \mathcal{F}_{\text{d}, i-\frac{1}{2}}(\hat{u}_i, \hat{u}_{i+1}) \right] + \left[\mathcal{F}_{\text{c}, i+\frac{1}{2}}(\hat{u}_i, \hat{u}_{i+1}) - \mathcal{F}_{\text{c}, i-\frac{1}{2}}(\hat{u}_i, \hat{u}_{i+1}) \right] - h_i f_i. \quad (6)$$

It results that the numerical solution of system (4), (5) or (6) is the solution U of the affine problem

$$G^\alpha(U; u_{\text{lf}}, u_{\text{rg}}, f, \mathbf{d}) = (0, \dots, 0)^t.$$

Remark 1. *To determine the numerical solution, we recast the problem as a linear system of equations in the form $Ax = b$. To this end, we first determine the right-hand side term setting $b := G^\alpha(0; u_{\text{lf}}, u_{\text{rg}}, f, \mathbf{d})$. We then determine column A_i with $A_i := G^\alpha(e_i; u_{\text{lf}}, u_{\text{rg}}, f, \mathbf{d}) - b$, e_i being the canonical vector, $i = 1, \dots, I$. For the sake of simplicity, we employ a direct method solving the linear system allowing to evaluate the conditioning number of the system $k(A)$. Of course, iterative method like Krylov method will be more efficient for larger system.*

5. Numerical tests

To highlight the effectiveness and robustness of the scheme we detail five tests dedicated to each specific aspect of the method: the choice of the reconstruction, strong Peclet number, pure convective or diffusive problems, robustness of the scheme with non-uniform meshes, and diffusion equation with non-constant coefficients. Note that NA means "not applicable" in the tables.

5.1. Error measurements

In the following, $\|U\|_\infty = \max_{i=1,\dots,I} |u_i|$ represents the L^∞ norm of vector U . Note that we intentionally use the L^∞ norm since we deal with regular functions.

We first measure the consistency error of the schemes to observe the rate of convergence using the exact solution in the algorithm. For the Patankar scheme, the consistency error is given by

$$E_C(\bar{U}) := \|A^P \bar{U} - F - F_D\|_\infty,$$

while we introduce the consistency error for the three schemes G^α , $\alpha = 1, 2, 3$, by

$$E_C(\bar{U}) := \left\| G^\alpha(\bar{U}; u_{\text{lf}}, u_{\text{rg}}, f, \mathbf{d}) \right\|_\infty,$$

where

$$\bar{U} := (\bar{u}_1, \dots, \bar{u}_I), \quad \bar{u}_i := \frac{1}{h_i} \int_{K_i} u \, dx,$$

are the exact mean values of the solution of the continuous problem.

The error between the solution and its approximations is provided with L^∞ norm, namely

$$E_0 := \max_{i=1}^I |u_i - \bar{u}_i|.$$

Note that E_0 does not depend on the polynomial reconstruction but on the mean values.

Since diffusive flux use derivatives at the interface, we introduce E_1 as the L^∞ error of the derivative. For the G^α schemes, we use the polynomial reconstruction, setting

$$E_1(\mathbf{u}) := \max_{i=1}^I \left\{ \left| u'_i(x_{i-\frac{1}{2}}) - u'(x_{i-\frac{1}{2}}) \right|, \left| u'_i(x_{i+\frac{1}{2}}) - u'(x_{i+\frac{1}{2}}) \right| \right\}.$$

With such a definition, we measure the error of the derivatives with $E_1(\check{u})$ and $E_1(\tilde{u})$ for scheme G^1 and G^2 respectively. For the third scheme, we use $E_1(\tilde{u})$ since we have to compare the derivative approximation with the true derivative at the interface which only involves polynomials \tilde{u} . For the Patankar scheme, we provide an approximation of the derivative using the divided differences.

5.2. Example 1

In the first test, we consider the very simple convection diffusion problem with constant diffusion and velocity coefficients setting $a = 1$, $v = 1$ and $u_{\text{lf}} = 1$, $u_{\text{rg}} = e$ on the boundary while $f = 0$. The exact solution is $u(x) = \exp(x)$. Computations are carried out on uniform meshes ($h_r = 1$) of I cells with $I = 10, 20, 40, 80$ respectively. We plot in Figure 2 the convergence curves for the G^3 scheme while we display in Tables 1, 2, and 3 the errors E_C , E_0 , and E_1 with their respective convergence rate for the three schemes.

- The G^1 scheme
 - Error E_C . All the reconstructions achieve the expected optimal order d . Indeed, we can not expect a $d + 1$ convergence rate since only polynomial derivatives appear in the diffusive flux expression.
 - Error E_0 . For the \mathbb{P}_1 , \mathbb{P}_3 , and \mathbb{P}_5 reconstruction, we are close to the optimal order convergence with 2, 4, and 6 respectively, whereas we do not reach the expected optimal reconstruction and observe an accuracy discrepancy for the \mathbb{P}_2 and \mathbb{P}_4 reconstructions.
 - Error E_1 . All the reconstructions are close to the optimal order convergence for the derivative approximations.
 - The conditioning number of the matrices increases with the reconstruction order and the number of cells.
- The G^2 scheme
 - The convergence rate is very similar to the case G^1 . We just remark that the \mathbb{P}_1 does not provide the expected convergence rate.
 - The conditioning numbers of matrices deriving from the G^2 scheme are slightly higher with respect to the G^1 scheme.
- The G^3 scheme
 - We obtain very similar results with the G^1 scheme and observe a discrepancy of the order of convergence for the \mathbb{P}_1 reconstruction.
 - Matrices conditioning number are equal to the case G^2 .

– Convergence curves are linear providing clear convergence rates.

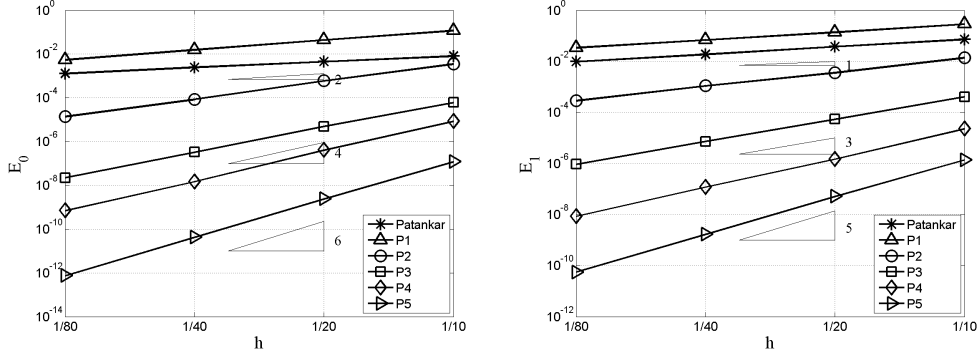


Figure 2: The G^3 scheme: convergence curves of E_0 (left) and E_1 (right).

5.3. Example 2

We now consider a similar convection diffusion problem with a large Peclet number setting $a = 1$ and $v = 10000$ with the same boundary conditions as Example 1 and uniform meshes. We set $f(x) = 9999 \exp(x)$ in order to find again the solution $u(x) = \exp(x)$.

We give in Tables 4 and 5 the errors E_C , E_0 , and E_1 with their respective convergence rate for the two schemes G^2 and G^3 . Clearly, the Patankar scheme does not provide a good solution while the PRO-schemes achieve the expected convergence order. Note that the discretisation of the convective term in the Patankar scheme is mainly responsible of the order discrepancy and could be improved using a MUSCL technique up to a second-order one.

5.4. Example 3

In the third test, we simulate a pure convection problem on uniform meshes setting $a = 0$, $v = 1$, $f(x) = \exp(x)$, and the inflow condition $u_{\text{if}} = 1$. Note that the outflow condition $u_{\text{rg}} = e$ should not be prescribed. Nevertheless, by construction of operator G^2 , we have to define a Dirichlet condition at $x = 1$ and we introduce the right outflow condition $u_{\text{rg}} = e$ compatible with the solution. To observe the scheme dependency on the extra condition, we also test the method using an arbitrary value for the outflow condition setting $u_{\text{rg}} = 100$.

Table 6 shows the E_C and E_0 errors with their respective convergence rate for schemes G^2 and G^3 using the extra condition $u_{\text{rg}} = e$ while Table 7

presents that errors for the same two schemes with the outflow condition $u_{\text{rg}} = 100$. Clearly, scheme G^2 provides wrong results in the last case since the convective flux uses a polynomial reconstruction which include the Dirichlet condition. Such a reconstruction does not make sense for the convective flux for outgoing velocity. Scheme G^3 is more relevant because polynomials \hat{u}_i are independent of the boundaries condition we observe a good convergence rate even with an arbitrary outflow condition.

5.5. Example 4

We address in the present test the scheme robustness problem with respect to the mesh with large form factor. Once again we consider the simple convection-diffusion problem with $\text{Pe}=1$ as Example 1 and $\text{Pe}=10000$ as Example 2 but using irregular meshes with $h_r = 20$.

Table 8 gives the E_0 and E_1 errors and their respective convergence rates with $\text{Pe}=1$, while Table 9 provides the same informations for $\text{Pe}=10000$. We achieve a very good convergence order for the \mathbb{P}_3 and \mathbb{P}_5 reconstructions with the optimal convergence rate both for small and large Peclet numbers.

5.6. Example 5

The last example is dedicated to the convection diffusion problem with non-constant coefficients. We only treat the diffusive part of the operator for the sake of simplicity setting $a(x) = \frac{1}{3 + 2 \cos(2\pi x)}$ and $v = 0$ with the right-hand side term $f(x) = 1$ and the boundary conditions $u_{\text{f}} = 0$ and $u_{\text{rg}} = 10$.

Tables 10 and 11 give the E_0 error and its respective convergence rates using uniform meshes and meshes with the form factor $h_r = 20$ respectively. We plot the convergence curves of E_0 in Figure 3 for the non-uniform mesh.

The Patankar scheme provides a second-order method since the convective part is removed. The G^3 scheme achieves very good convergence rate both for the uniform and the non-uniform meshes for the \mathbb{P}_3 and \mathbb{P}_5 reconstruction while the algorithm order is reduced of one order for \mathbb{P}_2 and \mathbb{P}_4 . Indeed, we expect a third-order scheme for the \mathbb{P}_2 whereas we obtain an effective second-order scheme with the numerical simulations. We observe a similar behavior with the \mathbb{P}_4 polynomial reconstruction.

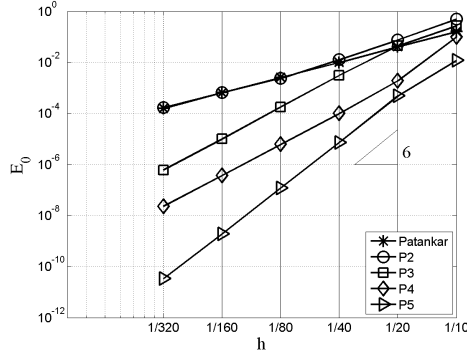


Figure 3: Regular coefficient case: convergence curves for E_0 and $h_r = 20$.

6. Conclusion

We have presented a new finite volume method for one-dimensional convection-diffusion problem which provides very high-order accuracy. Numerical simulations have been carried out to prove the capacity of the method to effectively reach the sixth-order accuracy. Several extensions are under consideration. The two- and three-dimensional case is of course of crucial importance, but we will also investigate the schemes for both Dirichlet and Neumann boundary conditions. Another difficulty concerns the solution stability when dealing with rough data. A strategy based on the MOOD method ([6, 7]) is currently being developed.

Acknowledgements: This research was financed by FEDER Funds through Programa Operacional Factores de Competitividade — COMPETE and by Portuguese Funds through FCT — Fundação para a Ciência e a Tecnologia, within the Project PEst-C/MAT/UI0013/2011.

7. Bibliography

References

- [1] F. Brezzi, K. Lipnikov, and M. Shashkov, Convergence of Mimetic Finite Difference Methods for Diffusion Problems on Polyhedral Meshes, *SIAM J. Num. Anal.*, 43 (2005), pp. 1872–1896.
- [2] Z. Cai, On the finite volume element method, *Numer. Math.* 58 (1991), pp. 713–735.
- [3] Z. Cai, J. Mandel, and S. Mc Cormick, The finite volume element method for diffusion equations on general triangulations, *SIAM J. Numer. Anal.* 28 (2) (1991), pp. 392–402.

- [4] A. Cangiani and G. Manzini, Flux reconstruction and solution post-processing in mimetic finite difference methods, *Computer Methods in Applied Mechanics and Engineering*, 197 (9-12) (2008), pp. 933-945.
- [5] Z. Chen, *Finite element methods and their applications* Springer-Verlag, (2005).
- [6] S. Clain, S. Diot, and R. Loubère, A high-order polynomial finite volume method for hyperbolic system of conservation laws with Multi-dimensional Optimal Order Detection (MOOD), *Journal of Computational Physics*, 230 (2011), pp. 4028–4050.
- [7] S. Clain, S. Diot, and R. Loubère, Multi-dimensional Optimal Order Detection (MOOD) — A very high-order Finite Volume Scheme for conservation laws on unstructured meshes, *Proceeding for the sixth Finite Volume and Complex Application*, Springer Verlag Editor, 1 (2011), pp. 263–271.
- [8] Y. Coudière, J.P. Vila, and P. Villedieu, Convergence rate of a finite volume scheme for a two dimensional convection diffusion problem, *Modél. Math. Anal. Numér.* 33 (3) (1999), pp. 493–516.
- [9] Y. Coudière and P. Villedieu, Convergence rate of a finite volume scheme for the linear convection-diffusion equation on locally refined meshes, *M2AN Math. Model. Numer. Anal.* 34 (6) (1999), pp. 1123–1149.
- [10] Y. Coudière and G. Manzini, The discrete duality finite volume method for convection-diffusion problems *SIAM j. numer. anal.* 47 (6) (2010), pp. 4163–4192.
- [11] J. Droniou and R. Eymard, A mixed finite volume scheme for anisotropic diffusion problems on any grid, *Numer. Math.*, 105 (2006), pp. 35–71.
- [12] K. Domelevo and P. Omnes, A finite volume method for the Laplace equation on almost arbitrary two-dimensional grids, *M2AN Math. Model. Numer. Anal.*, 39 (2005), pp. 1203–1249.
- [13] R. Eymard, T. Gallouët, and R. Herbin, The finite volume method, *Handbook for Numerical Analysis*, Ph. Ciarlet J.L. Lions eds., North Holland, (2000), pp. 715–1022.
- [14] R. Eymard, T. Gallouët, and R. Herbin, Finite volume approximation of elliptic problems and convergence of an approximate gradient, *Applied Numerical Mathematics* 37 (2001), pp. 31–53.
- [15] R. Eymard, T. Gallouët, and R. Herbin. Benchmark on Anisotropic Problems. SUSHI: a scheme using stabilization and hybrid interfaces for anisotropic heterogeneous diffusion problems, *FVCA5 — Finite Volumes for Complex Applications V* (2008), Wiley, pp. 801–814.
- [16] C. Grossmann, H.-G. Roos, and M. Stynes, *Numerical treatment of partial differential equations*, Springer-Verlag, (2007).
- [17] F. Hermeline, A finite volume method for the approximation of diffusion operators on distorted meshes, *J. Comput. Phys.*, 160 (2000), pp. 481–499.
- [18] G. Manzini and A. Russo, A finite volume method for advection-diffusion problems in convection-dominated regimes, *Comput. Methods Appl. Mech. Engrg.* 197 (2008), pp. 1242–1261
- [19] S. V. Patankar, *Numerical Heat Transfer and Fluid Flow*, Series in Computational Methods in Mechanics and Thermal Sciences, McGraw Hill, New York, (1980).
- [20] A. A. Samarskii, On monotone difference schemes for the elliptic and parabolic equations in the case of a non-self-adjoint elliptic operator, *Zh. Vychisl. Mat. i Mat. Fiz.* 5 (1965), pp. 548–551 (in Russian).

- [21] A. N. Tichonov and A. A. Samarskii, Homogeneous difference schemes on nonuniform nets, Zh. Vychisl. Mat. i Mat. Fiz. 2 (1962), pp. 812–832 (in Russian).
[22] A. Tveito, R. Winther, Introduction to partial differential equations: a computational approach Springer-Verlag, (1998).

Table 1: Example 1 — $u(x) = \exp(x)$, $a(x) = 1$, $v = 1$, $u_{lf} = 1$, $u_{rg} = e$, $h_r = 1$, G^1

	I	$k(A)$	E_C err	ord	E_0 err	ord	E_1 err	ord
Patankar	10	4.0E+01	7.8E−02	NA	8.3E−03	NA	7.4E−02	NA
	20	1.6E+02	4.2E−02	0.9	4.6E−03	0.8	3.8E−02	1.0
	40	6.4E+02	2.2E−02	0.9	2.5E−03	0.9	1.9E−02	1.0
	80	2.6E+03	1.1E−02	1.0	1.3E−03	1.0	9.8E−03	1.0
$\mathbb{P}_1(3)$	10	1.1E+01	1.6E−01	NA	4.1E−02	NA	1.7E−01	NA
	20	4.2E+01	8.2E−02	1.0	1.1E−02	1.9	7.9E−02	1.1
	40	1.6E+02	4.2E−02	1.0	2.9E−03	1.9	3.8E−02	1.1
	80	6.4E+02	2.1E−02	1.0	7.6E−04	2.0	1.8E−02	1.0
$\mathbb{P}_2(5)$	10	1.1E+01	2.2E−02	NA	3.2E−03	NA	1.1E−02	NA
	20	4.1E+01	6.0E−03	1.9	5.2E−04	2.6	3.3E−03	1.7
	40	1.6E+02	1.6E−03	1.9	7.4E−05	2.8	9.6E−04	1.8
	80	6.3E+02	4.0E−04	2.0	1.4E−05	2.4	2.6E−04	1.9
$\mathbb{P}_3(5)$	10	3.5E+01	1.0E−03	NA	5.9E−05	NA	4.0E−04	NA
	20	1.4E+02	1.4E−04	2.9	4.7E−06	3.6	5.5E−05	2.9
	40	5.4E+02	1.8E−05	2.9	3.3E−07	3.8	7.3E−06	2.9
	80	2.2E+03	2.4E−06	3.0	2.2E−08	3.9	9.3E−07	3.0
$\mathbb{P}_4(7)$	10	3.6E+01	1.5E−04	NA	7.8E−06	NA	1.3E−05	NA
	20	1.4E+02	1.1E−05	3.8	3.9E−07	4.3	1.5E−06	3.1
	40	5.6E+02	7.3E−07	3.9	1.5E−08	4.7	1.2E−07	3.6
	80	2.2E+03	4.7E−08	4.0	7.0E−10	4.4	8.6E−09	3.8
$\mathbb{P}_5(7)$	10	6.9E+01	4.7E−06	NA	9.9E−08	NA	1.4E−06	NA
	20	2.7E+02	1.7E−07	4.8	2.3E−09	5.5	5.2E−08	4.8
	40	1.1E+03	5.6E−09	4.9	4.2E−11	5.8	1.7E−09	4.9
	80	4.3E+03	1.8E−10	5.0	8.1E−13	5.7	5.6E−11	4.9

Table 2: Example 1 — $u(x) = \exp(x)$, $a(x) = 1$, $v = 1$, $u_{lf} = 1$, $u_{rg} = e$, $h_r = 1$, G^2

	I	$k(A)$	E_C err	ord	E_0 err	ord	E_1 err	ord
Patankar	10	4.0E+01	7.8E−02	NA	8.3E−03	NA	7.4E−02	NA
	20	1.6E+02	4.2E−02	0.9	4.6E−03	0.8	3.8E−02	1.0
	40	6.4E+02	2.2E−02	0.9	2.5E−03	0.9	1.9E−02	1.0
	80	2.6E+03	1.1E−02	1.0	1.3E−03	1.0	9.8E−03	1.0
$\mathbb{P}_1(3)$	10	1.8E+01	1.8E−01	NA	1.4E−01	NA	3.2E−01	NA
	20	5.3E+01	9.1E−02	1.0	4.9E−02	1.5	1.5E−01	1.1
	40	1.8E+02	4.6E−02	1.0	1.7E−02	1.5	7.3E−02	1.1
	80	6.7E+02	2.3E−02	1.0	5.8E−03	1.5	3.5E−02	1.0
$\mathbb{P}_2(5)$	10	1.2E+01	2.5E−02	NA	3.9E−03	NA	1.5E−02	NA
	20	4.2E+01	6.6E−03	1.9	6.2E−04	2.7	3.6E−03	2.1
	40	1.6E+02	1.7E−03	1.9	8.6E−05	2.8	1.1E−03	1.7
	80	6.4E+02	4.4E−04	2.0	1.4E−05	2.7	3.0E−04	1.9
$\mathbb{P}_3(5)$	10	3.7E+01	9.7E−04	NA	6.0E−05	NA	4.0E−04	NA
	20	1.4E+02	1.3E−04	2.9	4.7E−06	3.7	5.5E−05	2.9
	40	5.7E+02	1.7E−05	2.9	3.3E−07	3.9	7.2E−06	2.9
	80	2.3E+03	2.2E−06	3.0	2.2E−08	3.9	9.3E−07	3.0
$\mathbb{P}_4(7)$	10	3.8E+01	1.4E−04	NA	8.0E−06	NA	1.2E−05	NA
	20	1.5E+02	1.0E−05	3.8	4.0E−07	4.3	1.5E−06	3.0
	40	5.9E+02	6.8E−07	3.9	1.5E−08	4.7	1.2E−07	3.6
	80	2.4E+03	4.4E−08	4.0	7.0E−10	4.4	8.6E−09	3.8
$\mathbb{P}_5(7)$	10	7.0E+01	4.4E−06	NA	1.0E−07	NA	1.4E−06	NA
	20	2.8E+02	1.6E−07	4.8	2.3E−09	5.5	5.2E−08	4.8
	40	1.1E+03	5.3E−09	4.9	4.2E−11	5.8	1.7E−09	4.9
	80	4.4E+03	1.7E−10	5.0	7.5E−13	5.8	5.6E−11	4.9

Table 3: Example 1 — $u(x) = \exp(x)$, $a(x) = 1$, $v = 1$, $u_{lf} = 1$, $u_{rg} = e$, $h_r = 1$, G^3

	I	$k(A)$	E_C err	ord	E_0 err	ord	E_1 err	ord
Patankar	10	4.0E+01	7.8E−02	NA	8.3E−03	NA	7.4E−02	NA
	20	1.6E+02	4.2E−02	0.9	4.6E−03	0.8	3.8E−02	1.0
	40	6.4E+02	2.2E−02	0.9	2.5E−03	0.9	1.9E−02	1.0
	80	2.6E+03	1.1E−02	1.0	1.3E−03	1.0	9.8E−03	1.0
$\mathbb{P}_1(3)$	10	1.7E+01	1.7E−01	NA	1.2E−01	NA	2.9E−01	NA
	20	5.2E+01	8.9E−02	0.9	4.5E−02	1.4	1.4E−01	1.0
	40	1.8E+02	4.6E−02	1.0	1.6E−02	1.5	7.0E−02	1.0
	80	6.7E+02	2.3E−02	1.0	5.6E−03	1.5	3.5E−02	1.0
$\mathbb{P}_2(5)$	10	1.1E+01	2.4E−02	NA	3.6E−03	NA	1.4E−02	NA
	20	4.1E+01	6.5E−03	1.9	6.0E−04	2.6	3.6E−03	2.0
	40	1.6E+02	1.7E−03	1.9	8.5E−05	2.8	1.1E−03	1.7
	80	6.4E+02	4.4E−04	2.0	1.4E−05	2.6	2.9E−04	1.9
$\mathbb{P}_3(5)$	10	3.7E+01	8.8E−04	NA	6.2E−05	NA	4.1E−04	NA
	20	1.5E+02	1.3E−04	2.8	4.9E−06	3.7	5.5E−05	2.9
	40	5.7E+02	1.7E−05	2.9	3.3E−07	3.9	7.3E−06	2.9
	80	2.3E+03	2.2E−06	3.0	2.2E−08	3.9	9.3E−07	3.0
$\mathbb{P}_4(7)$	10	3.9E+01	1.3E−04	NA	8.5E−06	NA	2.3E−05	NA
	20	1.5E+02	9.7E−06	3.7	4.1E−07	4.4	1.5E−06	3.9
	40	5.9E+02	6.6E−07	3.9	1.5E−08	4.7	1.2E−07	3.7
	80	2.4E+03	4.3E−08	3.9	7.0E−10	4.5	8.6E−09	3.8
$\mathbb{P}_5(7)$	10	7.2E+01	3.8E−06	NA	1.2E−07	NA	1.4E−06	NA
	20	2.8E+02	1.5E−07	4.7	2.4E−09	5.6	5.2E−08	4.8
	40	1.1E+03	5.1E−09	4.8	4.3E−11	5.8	1.7E−09	4.9
	80	4.4E+03	1.6E−10	5.0	7.6E−13	5.8	5.6E−11	4.9

Table 4: Example 2 — $u(x) = \exp(x)$, $a(x) = 1$, $v = 10000$, $u_{\text{lf}} = 1$, $u_{\text{rg}} = e$, $h_r = 1$, G^2

	I	$k(A)$	$E_{\mathcal{C}}$ err	ord	E_0 err	ord	E_1 err	ord
Patankar	10	1.3E+01	5.3E+02	NA	1.3E−01	NA	2.7E+00	NA
	20	2.6E+01	2.6E+02	1.0	6.6E−02	1.0	2.7E+00	0.0
	40	5.2E+01	1.3E+02	1.0	3.3E−02	1.0	2.7E+00	0.0
	80	1.0E+02	6.3E+01	1.0	1.7E−02	1.0	2.7E+00	0.0
$\mathbb{P}_1(3)$	10	1.3E+01	5.0E+01	NA	5.8E−03	NA	2.1E−01	NA
	20	2.6E+01	1.2E+01	2.0	1.5E−03	1.9	1.1E−01	1.0
	40	5.1E+01	3.1E+00	2.0	3.9E−04	2.0	5.4E−02	1.0
	80	1.0E+02	7.6E−01	2.0	9.6E−05	2.0	2.7E−02	1.0
$\mathbb{P}_2(5)$	10	1.3E+01	7.9E+00	NA	7.5E−04	NA	2.3E−02	NA
	20	2.5E+01	1.1E+00	2.9	1.1E−04	2.8	6.1E−03	1.9
	40	5.0E+01	1.3E−01	3.0	1.4E−05	2.9	1.6E−03	1.9
	80	1.0E+02	1.7E−02	3.0	1.8E−06	3.0	4.0E−04	2.0
$\mathbb{P}_3(5)$	10	2.1E+01	2.9E−01	NA	2.4E−05	NA	4.9E−04	NA
	20	3.5E+01	2.0E−02	3.9	1.7E−06	3.9	6.4E−05	3.0
	40	6.3E+01	1.3E−03	3.9	1.1E−07	3.9	8.0E−06	3.0
	80	1.2E+02	8.3E−05	4.0	7.0E−09	4.0	9.9E−07	3.0
$\mathbb{P}_4(7)$	10	1.9E+01	4.1E−02	NA	2.9E−06	NA	9.1E−05	NA
	20	3.2E+01	1.5E−03	4.8	1.1E−07	4.8	6.3E−06	3.9
	40	5.7E+01	5.0E−05	4.9	3.6E−09	4.9	4.1E−07	3.9
	80	1.1E+02	1.6E−06	5.0	1.2E−10	4.9	2.7E−08	4.0
$\mathbb{P}_5(7)$	10	8.6E+01	1.6E−03	NA	1.0E−07	NA	2.0E−06	NA
	20	1.2E+02	2.9E−05	5.8	1.7E−09	5.9	7.4E−08	4.7
	40	1.6E+02	4.8E−07	5.9	2.7E−11	5.9	2.5E−09	4.9
	80	2.1E+02	8.1E−09	5.9	3.9E−13	6.1	6.5E−11	5.2

Table 5: Example 2 — $u(x) = \exp(x)$, $a(x) = 1$, $v = 10000$, $u_{\text{lf}} = 1$, $u_{\text{rg}} = e$, $h_r = 1$, G^3

	I	$k(A)$	$E_{\mathcal{C}}$ err	ord	E_0 err	ord	E_1 err	ord
Patankar	10	1.3E+01	5.3E+02	NA	1.3E−01	NA	2.7E+00	NA
	20	2.6E+01	2.6E+02	1.0	6.6E−02	1.0	2.7E+00	0.0
	40	5.2E+01	1.3E+02	1.0	3.3E−02	1.0	2.7E+00	0.0
	80	1.0E+02	6.3E+01	1.0	1.7E−02	1.0	2.7E+00	0.0
$\mathbb{P}_1(3)$	10	1.3E+01	1.1E+02	NA	6.4E−03	NA	1.6E−01	NA
	20	2.6E+01	2.9E+01	1.9	1.8E−03	1.8	8.5E−02	0.9
	40	5.1E+01	7.5E+00	2.0	4.8E−04	1.9	4.4E−02	1.0
	80	1.0E+02	1.9E+00	2.0	1.2E−04	2.0	2.2E−02	1.0
$\mathbb{P}_2(5)$	10	1.3E+01	1.8E+01	NA	1.6E−03	NA	2.4E−02	NA
	20	2.5E+01	2.4E+00	2.9	2.0E−04	3.0	6.3E−03	1.9
	40	5.0E+01	3.1E−01	2.9	2.6E−05	3.0	1.6E−03	2.0
	80	1.0E+02	4.0E−02	3.0	3.3E−06	3.0	4.1E−04	2.0
$\mathbb{P}_3(5)$	10	1.8E+01	1.1E+00	NA	7.2E−05	NA	8.2E−04	NA
	20	3.6E+01	7.9E−02	3.9	4.5E−06	4.0	1.1E−04	2.9
	40	7.2E+01	5.2E−03	3.9	2.8E−07	4.0	1.5E−05	2.9
	80	1.4E+02	3.3E−04	4.0	1.8E−08	4.0	1.9E−06	3.0
$\mathbb{P}_4(7)$	10	2.0E+01	1.7E−01	NA	1.0E−05	NA	3.4E−04	NA
	20	3.9E+01	6.0E−03	4.8	3.1E−07	5.1	2.1E−05	4.0
	40	7.7E+01	2.0E−04	4.9	9.6E−09	5.0	1.3E−06	4.0
	80	1.5E+02	6.5E−06	5.0	3.0E−10	5.0	8.2E−08	4.0
$\mathbb{P}_5(7)$	10	4.1E+01	7.3E−03	NA	3.1E−07	NA	5.3E−06	NA
	20	7.6E+01	1.3E−04	5.8	4.8E−09	6.0	1.6E−07	5.0
	40	1.5E+02	2.2E−06	5.9	7.3E−11	6.0	4.6E−09	5.1
	80	2.9E+02	3.7E−08	5.9	1.1E−12	6.0	1.4E−10	5.0

Table 6: Example 3 — $f(x) = \exp(x)$, $a(x) = 0$,
 $v = 1$, $u_{\text{lf}} = 1$ ($u_{\text{rg}} = e$), $h_r = 1$, $\mathbb{P}_3(5)$

	I	$E_{\mathcal{C}}$		E_0	
		err	ord	err	ord
G^2	10	2.9E−05	NA	2.4E−05	NA
	20	2.0E−06	3.9	1.7E−06	3.8
	40	1.3E−07	3.9	1.1E−07	3.9
	80	8.5E−09	4.0	7.1E−09	4.0
G^3	10	1.1E−04	NA	7.2E−05	NA
	20	7.9E−06	3.9	4.5E−06	4.0
	40	5.2E−07	3.9	2.8E−07	4.0
	80	3.3E−08	4.0	1.8E−08	4.0

Table 7: Example 3 — $f(x) = \exp(x)$, $a(x) = 0$,
 $v = 1$, $u_{\text{lf}} = 1$ ($u_{\text{rg}} = 100$), $h_r = 1$, $\mathbb{P}_3(5)$

	I	$E_{\mathcal{C}}$		E_0	
		err	ord	err	ord
G^2	10	8.1E+01	NA	1.7E+02	NA
	20	8.1E+01	0.0	1.7E+02	0.0
	40	8.1E+01	0.0	1.7E+02	0.0
	80	8.1E+01	0.0	1.7E+02	0.0
G^3	10	1.1E−04	NA	7.2E−05	NA
	20	7.9E−06	3.9	4.5E−06	4.0
	40	5.2E−07	3.9	2.8E−07	4.0
	80	3.3E−08	4.0	1.8E−08	4.0

Table 8: Example 4 — $u(x) = \exp(x)$, $a(x) = 1$, $v = 1$, $u_{\text{lf}} = 1$ ($u_{\text{rg}} = e$), $h_r = 20$, G^3

	I	E_0 err	ord	E_1 err	ord
Patankar	10	9.6E-03	NA	1.6E-01	NA
	20	5.0E-03	0.9	8.6E-02	0.9
	40	2.5E-03	1.0	4.4E-02	1.0
	80	1.3E-03	1.0	2.2E-02	1.0
$\mathbb{P}_3(5)$	10	3.5E-04	NA	1.2E-03	NA
	20	4.5E-05	2.9	1.6E-04	2.9
	40	4.3E-06	3.4	2.1E-05	3.0
	80	3.5E-07	3.6	2.6E-06	3.0
$\mathbb{P}_5(7)$	10	8.5E-07	NA	2.5E-06	NA
	20	1.7E-08	5.7	8.3E-08	4.9
	40	3.0E-10	5.8	2.8E-09	4.9
	80	4.9E-12	5.9	9.3E-11	4.9

Table 9: Example 4 — $u(x) = \exp(x)$, $a(x) = 1$, $v = 10000$, $u_{\text{lf}} = 1$, $u_{\text{rg}} = e$, $h_r = 20$, G^3

	I	E_0 err	ord	E_1 err	ord
Patankar	10	2.4E-01	NA	2.6E+00	NA
	20	1.2E-01	1.0	2.6E+00	0.0
	40	6.3E-02	1.0	2.5E+00	0.1
	80	3.2E-02	1.0	2.5E+00	0.0
$\mathbb{P}_3(5)$	10	3.2E-05	NA	1.6E-03	NA
	20	2.2E-06	3.9	1.7E-04	3.2
	40	1.4E-07	3.9	2.1E-05	3.1
	80	9.3E-09	3.9	2.5E-06	3.1
$\mathbb{P}_5(7)$	10	1.9E-07	NA	1.3E-05	NA
	20	2.6E-09	6.2	3.4E-07	5.2
	40	4.2E-11	6.0	9.9E-09	5.1
	80	6.8E-13	6.0	3.0E-10	5.0

Table 10: Example 5 — $f(x) = 1$,
 $a(x) = \frac{1}{3+2\cos(2\pi x)}$, $v = 0$, $u_{\text{f}} = 0$,
 $u_{\text{rg}} = 10$, $h_{\text{r}} = 1$, G^3

	I	E_0	ord
		err	
Patankar	10	4.4E−02	NA
	20	1.1E−02	2.0
	40	2.8E−03	2.0
	80	6.9E−04	2.0
	160	1.7E−04	2.0
	320	4.3E−05	2.0
	$\mathbb{P}_2(5)$	10	4.0E−01
20		4.9E−02	3.0
40		1.2E−02	2.1
80		3.0E−03	2.0
160		7.6E−04	2.0
320		2.0E−04	2.0
$\mathbb{P}_3(5)$		10	4.4E−02
	20	2.6E−03	4.1
	40	1.1E−04	4.5
	80	5.6E−06	4.4
	160	3.3E−07	4.1
	320	2.0E−08	4.0
	$\mathbb{P}_4(7)$	10	3.8E−02
20		1.4E−03	4.8
40		1.0E−04	3.8
80		6.7E−06	3.9
160		4.3E−07	4.0
320		2.7E−08	4.0
$\mathbb{P}_5(7)$		10	3.4E−03
	20	6.8E−05	5.6
	40	8.6E−07	6.3
	80	9.5E−09	6.5
	160	1.2E−10	6.3
	320	3.7E−12	5.0

Table 11: Example 5 — $f(x) = 1$,
 $a(x) = \frac{1}{3+2\cos(2\pi x)}$, $v = 0$, $u_{\text{f}} = 0$,
 $u_{\text{rg}} = 10$, $h_{\text{r}} = 20$, G^3

	I	E_0	ord
		err	
Patankar	10	1.6E−01	NA
	20	4.1E−02	1.9
	40	1.0E−02	2.0
	80	2.6E−03	2.0
	160	6.5E−04	2.0
	320	1.6E−04	2.0
$\mathbb{P}_2(5)$	10	4.9E−01	NA
	20	7.7E−02	2.7
	40	1.3E−02	2.5
	80	2.4E−03	2.5
	160	6.5E−04	1.9
	320	1.7E−04	1.9
$\mathbb{P}_3(5)$	10	2.7E−01	NA
	20	4.4E−02	2.6
	40	3.1E−03	3.8
	80	1.8E−04	4.1
	160	1.0E−05	4.1
	320	6.1E−07	4.1
$\mathbb{P}_4(7)$	10	9.8E−02	NA
	20	1.9E−03	5.7
	40	1.0E−04	4.2
	80	6.1E−06	4.1
	160	3.7E−07	4.0
	320	2.3E−08	4.0
$\mathbb{P}_5(7)$	10	1.2E−02	NA
	20	4.8E−04	4.7
	40	7.3E−06	6.0
	80	1.2E−07	5.9
	160	1.9E−09	6.0
	320	3.0E−11	6.0